Dalton Transactions

Accepted Manuscript

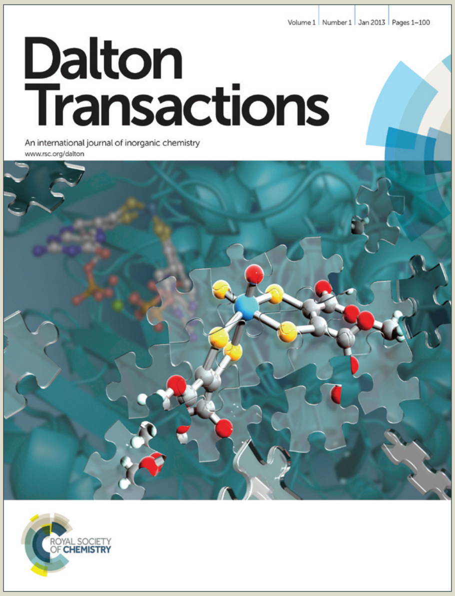

ROYAL SOCIETY OF CHEMISTRY

www.rsc.org/dalton

Dalton Transactions RSCPublishing

ARTICLE

Cite this: DOI: 10.1039/x0xx00000x

Received 00th January 2012,
Accepted 00th January 2012

DOI: 10.1039/x0xx00000x

www.rsc.org/

3D reconstruction of atomic structures from high angle annular dark field (HAADF) STEM images and its application on zeolite silicalite-1

Tom Willhammar,[a] Alvaro Mayoral[b] and Xiaodong Zou*[a] ,

High-resolution transmission electron microscopy (HRTEM) has shown to be very powerful for solving three-dimensional (3D) structures of unknown crystals. HRTEM has a unique advantage over diffraction for structure solution. Crystallographic structure factor phases, which are lost in diffraction, can be directly obtained from HRTEM images. For determination of a 3D crystalline structure by HRTEM, the crystallographic structure factor amplitudes and phases extracted from HRTEM images along different zone axes are combined to reconstruct a 3D electrostatic potential map. During the recent years, scanning transmission electron microscopy (STEM) has reached the atomic resolution which is comparable to that of HRTEM. Here we show for the first time that the structure factor phases can be also obtained from high angle annular dark-field (HAADF)-STEM images and used for 3D reconstruction of atomic structures. This is applied to the complex zeolite structure, silicalite-1 (Formula SiO_2, framework code MFI, *Pnma*, a = 20.090 Å, b = 19.738 Å and c = 13.142 Å). We have compared the amplitudes and phases obtained from HAADF-STEM images with those from HRTEM images.

Introduction

Structure determination is of outermost importance since it can give crucial insights into how a material is built on the atomic scale. The structure information is essential for understanding the properties of the material. Electron diffraction (ED) and high-resolution transmission electron microscopy (HRTEM) have shown to be very powerful for solving three-dimensional (3D) structures of unknown crystals. There are two main advantages of using electrons than X-rays for structure determination; 1) crystals too small to be studied by single crystal X-ray diffraction can be studied by electrons and 2) crystallographic structure factor phases, which are lost in diffraction, can be directly obtained from HRTEM images. The recently developed automated electron diffraction tomography (ADT) and the rotation electron diffraction (RED) have made the collection of complete 3D electron diffraction data much more feasible. The intensities obtained from ADT or RED can be directly used for structure solution.[1,2]

TEM images contain by definition only two-dimensional (2D) information of the sample, the three-dimensional structure of the sample is projected into a 2D image. In HRTEM imaging, the phase contrast from coherent electrons is utilized. The contrast in an HRTEM image depends not only on the structure projection of the specimen, but also on the crystal thickness and the TEM optics especially defocus and astigmatism of the objective lens. An HRTEM image is interpretable in terms of the projected electrostatic potential of the specimen if the crystal is thin enough to fulfill the weak phase object approximation and the image is taken under an optimum defocus condition, i.e. Scherzer focus.[3] For structure determination by HRTEM, the crystallographic structure factor amplitudes and phases are extracted from HRTEM images. The structure factors extracted from HRTEM images have been proven to be an important complement to powder X-ray diffraction for structure solution of complex zeolitic structures.[4-6]

For 3D structure determination by HRTEM, it is common to combine information from different projections. Crystallographic structure factor amplitudes and phases extracted from HRTEM images along different zone axes are combined to reconstruct a 3D electrostatic potential map, i.e. 3D reconstruction based on crystallographic image processing. To do this, the first step is to extract structure factors from the

Fourier transform (FT) of each of the acquired zone axis HRTEM images.[7] The structure factor amplitudes and phases are determined from the amplitudes and phases of the corresponding Fourier component in the FT.[8,9] The crystallographic structure factors $F(hkl)$ extracted from HRTEM images acquired along different projections can then be merged to create a 3D map representing the electrostatic potential distribution $\varphi(xyz)$ inside the crystal according to the following equation:

$$\varphi(xyz) = \frac{\lambda}{\sigma\Omega}\sum_{h,k,l} F(hkl)exp[-2\pi i(hx+ky+ly)] \qquad (1)$$

where Ω is the unit cell volume and σ the interaction constant. From a 3D potential map reconstructed from the most important projections, the atomic positions can be identified under conditions where the resolution of the original images is high enough.[3]

3D reconstruction of HRTEM images from different zone axes is limited to crystalline materials but it has shown to be powerful for determination of many structures that could not be solved by X-ray or electron diffraction. 3D reconstruction is the method of choice for very small crystals, complex structures and disordered materials. Among the structures solved by this method are complex quasicrystal approximants,[10] mixed metal compounds[11] and zeolite structures with high complexity or disorder.[12-15] For non-periodic objects, electron tomography is a general approach. However, the resolution has until recently been limited. Only in a few cases atomic resolution has been achieved, for simple structures and very stable materials.[16,17]

Until now, 3D reconstruction based on crystallographic image processing has been limited to HRTEM images. Scanning transmission electron microscopy (STEM) can also provide structural information at atomic level. For STEM, the probe is scanned in a raster over the sample by coils above the specimen. An annular dark field detector detects the electrons scattered at high angles to form high angle annular dark field (HAADF) images. The electrons detected by the HAADF detector are incoherent and the corresponding contrast is related to the atomic number and therefore called *Z* contrast. This contrast is normally easily interpreted as the projected atomic arrangement of the specimen. Recent developments in lens aberration correctors have improved the resolution of the STEM images into atomic scales. During the recent years STEM imaging has been used to study zeolites with great success.[18-21] In principle, it should be possible to reconstruct a 3D map by combining STEM images along different projections. However, STEM images with atomic resolution have to our knowledge not yet been used for 3D reconstruction.

Here we apply the 3D reconstruction on silicalite-1, which has the MFI zeolite framework and is one of the most complex zeolites.[22] We show for the first time that a 3D map of zeolite silicalite-1 can be reconstructed from high resolution high angle annular dark-field (HAADF)-STEM images taken along three main-zone axes, in the same way as the 3D reconstruction from HRTEM images. The plane group of the crystal projection can be determined from the HAADF-STEM images. The amplitudes and phases extracted from the HAADF-STEM images are compared to those of structure factors calculated from the structure model and those from HRTEM images.

Results and discussion

A. 3D reconstruction from STEM images

HAADF-STEM images from the three main zone axes, [010], [001] and [100] of the zeolite silicalite-1 were acquired (Fig. 1). For the crystallographic image analysis, Fourier transforms were calculated from each of the images. The resolution of the images is determined from the outmost spots in the Fourier transforms. The resolution in the three STEM images is in the range between 1.8 – 2.0 Å. The image resolution of zeolites is mainly limited by the beam damage of the sample, not by the performance of the microscope.

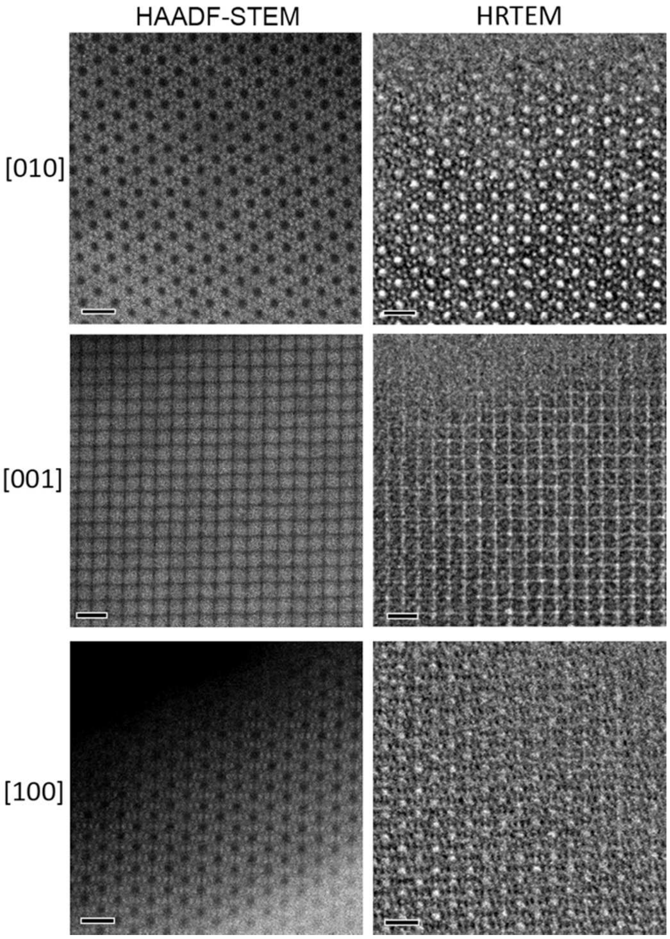

Fig. 1 Cs-corrected HAADF-STEM images (left) and HRTEM images (right) of silicalite-1 taken along the three main zone axes [010], [001] and [100]. The scale bars are 2 nm. Note that the contrast is reversed between the HAADF-STEM and the HRTEM images. The pores are black in the HAADF-STEM images and white in the HRTEM images.

From the Fourier transforms of the HAADF-STEM images (Fig. 2), the amplitude and phase for each reflection can be extracted. The amplitude is determined by an integration of the pixel amplitudes around the lattice point and the phase is taken from the pixel at the lattice point. By examining the amplitudes and phases of all the reflections, the projected symmetry of the structure can be determined. All projections contain some systematic absent reflections, which indicate the presence of centering, glide planes or screw axes. Since the phase relations are different for different plane groups, and all phases are restricted to either 0° or 180° for centrosymmetric plane groups, it is possible to determine the plane group of the projection by analyzing the phases. The origin is first moved to the place that fulfills best both the phase restrictions and phase relations for symmetry-related reflections, and then the phase residuals are compared for each symmetry (see Table S4). The plane group that fulfills the systematic absences and has the lowest phase residuals and highest possible symmetry is selected, which is *pgg* for [010], *pmg* for [001] and *cmm* for [100] projection. From the plane group symmetries, the space group *Pnma* was confirmed. The plane group symmetry is then imposed to the amplitudes and phases. The amplitudes of symmetry-related reflections are averaged and the phases are assigned to their closest value of 0° or 180°, as long as they are allowed by the phase relation of symmetry-related reflections used. Weak reflections do not give significant contribution to the 3D map. Fig. 3 shows the projected maps along the three main axes after crystallographic image processing, by imposing the projection symmetry onto each HAADF-STEM image. This is done by an inverse Fourier transform of the symmetry-imposed amplitudes and phases of reflections in Table S1-S3 according to Eqn. 1. All the potential maps clearly show a contrast that well resembles the structure projection.

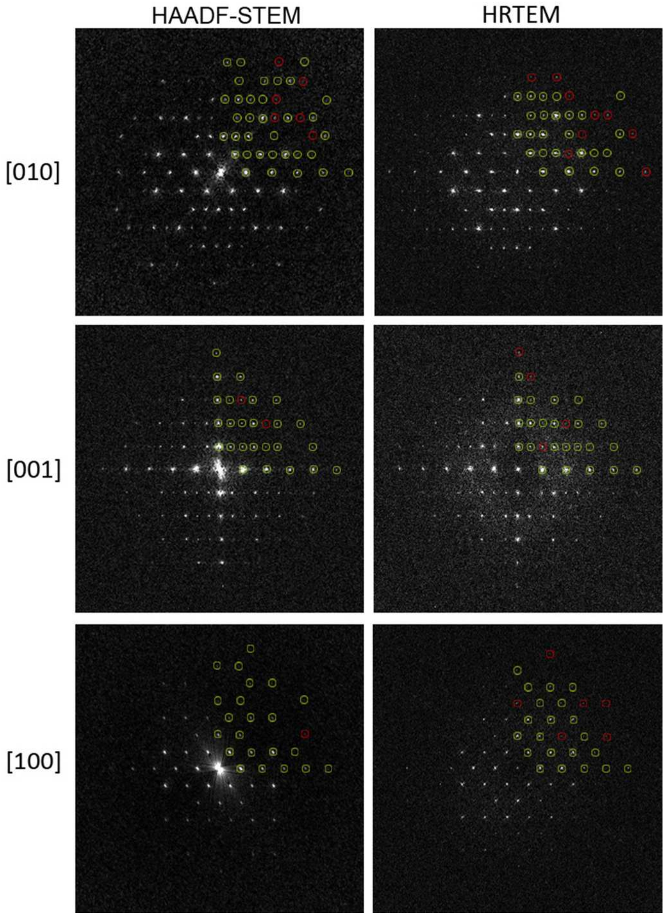

Fig. 2 Fourier transforms calculated from the HAADF-STEM (left) and HRTEM images (right) of silicalite-1 taken along the three main zone axes. The unique reflections with amplitudes larger than 2% of the strongest reflection are marked by circles. Yellow circles indicate correct phases and red circles wrong phases. The phases extracted from the HRTEM images are shifted by 180° compared to the calculated phases because of the reversed contrast. Note that the phases of most strong reflections are correct.

By combining the amplitudes and phases from the three data sets of the three main zone axes into one data set and performing an inverse Fourier transformation according to Eqn. 1, a 3D map can be constructed. The amplitudes of each of the three data sets were scaled against the amplitudes calculated from the structure model before merged into a three-dimensional data set. The origin for each projection was chosen based on the phases of the common reflections. The three-dimensional map constructed from the HAADF-STEM images shows good resemblance with the structure model of silicalite-1, see Fig. 4. The framework Si positions can be identified from the 3D map. Although O positions cannot be identified due to the resolution limit, they can be estimated because they are always between neighboring Si atoms. This shows that 3D reconstruction of the atomic structure from HAADF-STEM images is successful.

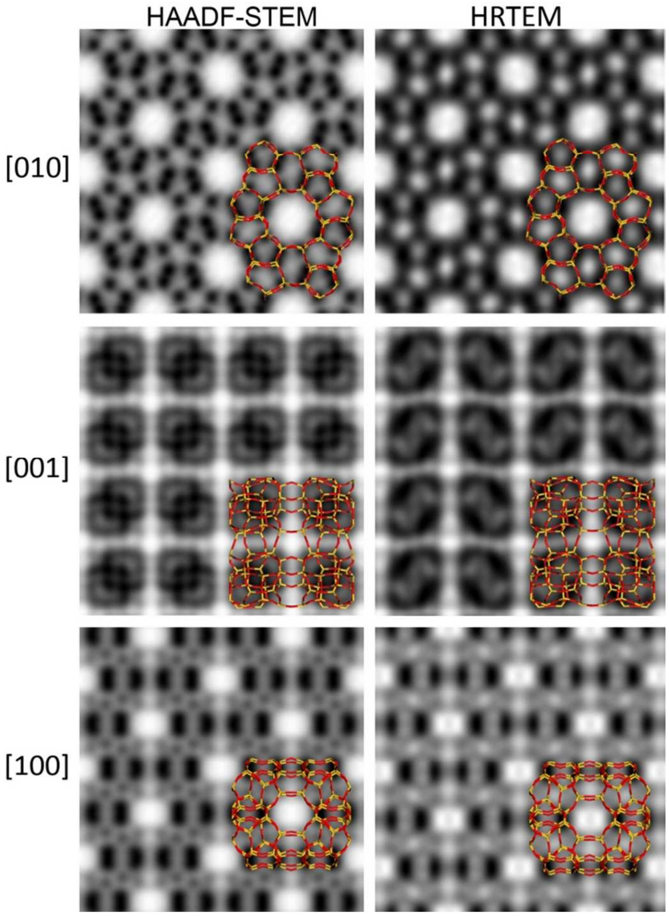

Fig. 3 Projected electrostatic potential maps calculated from the Fourier transforms from the HAADF-STEM (left) and HRTEM images (right) for the three main zone axes. The plane group symmetries determined from the images are applied. The symmetries are *pgg*, *pmg* and *cmm* for the [010], [001] and [100] respectively.

B. Comparison between HAADF-STEM and HRTEM images

In order to put the 3D reconstruction from the HAADF-STEM images in perspective, a similar 3D reconstruction was performed from HRTEM images taken along the three main zone axes of the same silicalite-1 material. The contrast of HRTEM images is reversed compared to that of HAADF-STEM images (Fig. 1), where the atoms are shown in black in HRTEM images and white in HAADF-STEM images. The resolution of the HRTEM and HAADF-STEM images is similar, as shown in the corresponding Fourier transforms in

Fig. 2. The low angle reflections near the direct beam in the Fourier transforms (FTs) of the HAADF-STEM images are stronger than those in the FTs of the HRTEM images. Out of the 15 strongest reflections in the Fourier transforms of each image, 12, 13 and 12 reflections are in common between the HAADF-STEM and HRTEM images for the projections along [010], [001] and [100], respectively.

The relative unit cell dimensions and the angles were determined from the positions of the reflections in the Fourier transforms of the HAADF-STEM and HRTEM images, respectively and listed in Table 1. Compared to those of the MFI zeolite framework in the Database of Zeolite Structures (*Pnma*, a = 20.090 Å, b = 19.738 Å and c = 13.142 Å),[22] the unit cell dimensions obtained from HAADF-STEM images differ on average by 0.60 Å, which is larger than the 0.41 Å average difference obtained for the HRTEM images. The angle distortions (up to 3.4°) are significantly larger in the HAADF-STEM images compared to those (up to 0.8°) in the HRTEM images. In conclusion, the lattice distortions are slightly larger in the HAADF-STEM images compared to the HRTEM images, which may be due to the spatial instability of the STEM and the specimen drift during the beam scan on the crystals.

Table 1 Comparison of the unit cell parameters determined from the experimental HAADF-STEM and HRTEM images taken along the three main zone axes. Those from the zeolite database are also given for comparison. The unit cell dimensions are scaled to have one unit cell dimension (indicated by *) to be the same as the one in the zeolite database.

		HAADF-STEM	HRTEM	Database	Δ(HAADF-STEM)	Δ(HRTEM)
[010]	**a* (Å)	20.09	20.09	20.09	-	-
	c (Å)	13.85	13.48	13.14	0.71	0.34
	β (°)	93.4	90.6	90.0	3.4	0.6
[001]	**a* (Å)	20.09	20.09	20.09	-	-
	b (Å)	20.17	20.40	19.74	0.43	0.66
	γ (°)	91.9	90.3	90.0	1.9	0.3
[100]	**b* (Å)	19.74	19.74	19.74	-	-
	c (Å)	12.47	13.36	13.14	0.67	0.22
	α (°)	91.1	90.8	90.0	1.1	0.8

Amplitudes and phases were extracted from both the STEM and HRTEM images. The amplitude and phase residuals between symmetry-related reflections are significantly lower for the HAADF-STEM images (Table S1), which makes the symmetry determination from HAADF-STEM images more reliable than that from HRTEM images. This indicates that HAADF-STEM imaging transfers the contrast of the specimen to the image with less distortion.

Tables S2-S4 compare the amplitudes and phases extracted from the HAADF-STEM and HRTEM images with those calculated from the structure model of silicalite-1 (MFI).[22] The number of correct phases in the Fourier transforms from the HAADF-STEM and HRTEM images for each of the three zone axes is summarized in Table 2. A general trend is that the HAADF-STEM images give correct phases for more reflections compared to the HRTEM images. All the reflections with the wrong phases are weak, two of them have amplitudes of ~10% of the strongest amplitude and the rest are less than 6% of the strongest reflection. The amplitudes extracted from the HRTEM images are more sensitive to the conditions under which the image is taken. An agreement factor *R* was calculated between the amplitudes extracted from the HAADF-STEM/HRTEM images and the structure factor amplitudes calculated from the structure model, which is 0.385 for the HRTEM images and 0.316 for the HAADF-STEM images. This shows that the amplitudes extracted from the HAADF-STEM images are slightly closer to the theoretical structure factor amplitudes. Since the location of the atoms is determined by the structure factor phases, the HAADF-STEM images are more accurate in determining the positions of the atoms than the HRTEM images.

The 2D maps constructed from the amplitudes and phases extracted from the HRTEM images are in good resemblance with the structure model, as shown in Fig. 3. However, features in the maps constructed from the HRTEM images are less discrete compared to those from the HAADF-STEM images. This is because the amplitudes of the high angle reflections are generally stronger and the phases are more accurate from the HAADF-STEM images.

Table 2 Number of correct structure factor phases compared with the total number of unique structure factors for the reflections with amplitudes larger than 2% of the strongest reflection.

	HAADF-STEM	HRTEM
[010]	31/37	25/35
[001]	25/27	23/27
[100]	22/23	21/27

The 3D maps constructed from both the HAADF-STEM and the HRTEM images are in good resemblance with the structure model of silicalite-1, see Fig. 4. The framework Si-atoms can be identified in both cases. However, peaks from the 3D map created from the HAADF-STEM images are better resolved and the atomic positions can be determined more accurately. It should be noted that the HRTEM images were acquired on a conventional high resolution TEM without C_s-correctors, while the HAADF-STEM images were taken on a more advanced TEM with probe-correctors. The conclusions from the comparison should be made with care.

The use of HAADF-STEM images in this study has several advantages over HRTEM images. The main advantage is that the contrast in HAADF-STEM images is easier to interpret compared to that of HRTEM images. The contrast of the HAADF-STEM images is better defined around the atomic positions. The amplitudes and phases extracted from the HAADF-STEM images are closer to the calculated structure factor amplitude and phases than those from the HRTEM images. This is why it is possible to apply 3D reconstruction of HAADF-STEM images for structure determination. It is also easier to determine the symmetry of the crystal from the HAADF-STEM images. The only drawback of the HAADF-STEM images is the large lattice distortion. For beam sensitive materials like zeolites, STEM imaging has the advantage that only the studied area is illuminated at each time and the other area of the crystal is not damaged at the same time. If care is taken to minimize the beam dose, HAADF-STEM imaging is well suited to study beam sensitive materials. Generally speaking, HAADF-STEM images are more suited for electron crystallographic studies over conventional HTEM images; even the difference is not very dramatic. Since HADADF-STEM images are formed by Z-contrast, this would make it possible to distinguish between metals and silicon in zeolites when metals are incorporated.[23] Future studies are needed to confirm this.

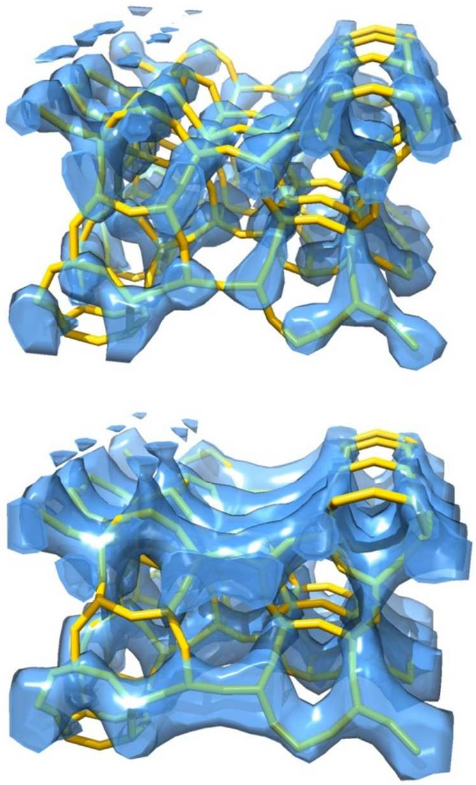

Fig. 4 The three-dimensional electrostatic potential maps of silicalite-1 reconstructed from the amplitudes and phases extracted from the Fourier transforms of (a) HAADF-STEM images and (b) HRTEM images taken along the three main zone axes.

Conclusions

We have shown for the first time that a 3D map of zeolite silicalite-1 at atomic level can be reconstructed from high resolution HAADF-STEM images taken along three main-zone axes, in the same way as the 3D reconstruction from HRTEM images. All the framework Si positions can be located from the 3D map. The plane group of the crystal projection can be determined from each HAADF-STEM image. The main advantage of STEM imaging is that the interpretation of the contrast is much easier compared to HRTEM imaging. The complexity of the data collection and interpretation for HRTEM images are avoided. In the case of silicalite-1, the amplitudes and phases extracted from HAADF-STEM images are slightly closer to the calculated crystallographic structure factor amplitudes and phases compared with those from HRTEM images. The phases extracted from HAADF-STEM images can be also helpful for structure solution by powder X-ray diffraction. One problem with HAADF-STEM images is the risk of geometrical distortions, which may be significantly improved with mechanically more stable stages. However, this can be taken care of by using electron diffraction or other diffraction techniques and symmetry evaluation to determine the lattice geometry. Our study also shows that HAADF-STEM images are also suitable for beam sensitive materials such as zeolites if care is taken to minimize the electron dose.

Experimental

The sample used for this study is the pure silica zeolite silicalite-1 which has an MFI-type framework. The ideal MFI framework has an orthorhombic symmetry and crystallizes in the space group *Pnma* with the lattice parameters a=20.090 Å, b=19.738 Å and c=13.142 Å [22]. The silicalite-1 crystals are ca 5 μm in size, which were first crushed in an agate mortar, then dispersed in ethanol and finally transferred onto a holey carbon grid for TEM observations.

For the STEM study, an X-FEG FEI Titan transmission electron microscope equipped with a monochromator and a CEOS spherical aberration (C_s) corrector for the electron probe was used. The HAADF-STEM images were collected at an accelerating voltage of 300 kV and a 50-200 mrad collection angles. Because silicalite-1 is electron beam sensitive, the monochromator was used in this study to decrease the beam current in order to minimize the beam damage.

HRTEM was performed at 200 kV using a JEOL JEM 2100F equipped with ultra-resolution polepieces (C_s=0.52 mm) and a Gatan CCD camera UltraScan 1000. HRTEM images were recorded from thin regions of the crystals at a defocus close to the Scherzer focus to ensure that the contrast corresponds to the projected potential of the specimen. Thin areas of the crystals were selected and crystallographic image processing was performed using the program CRISP.[8] Amplitudes and phases were extracted from the lattice points in the Fourier transforms of the selected areas. The calculated structure factor amplitudes and phases were obtained using the software eMap[24] from the ideal structure model of MFI in the Database of Zeolite Structures[22] using isotropic atomic displacement parameters U=0.015 Å^2 for silicon and U=0.03 Å^2 for oxygen.

Acknowledgements

This work was supported by the Swedish Research Council (VR), the Swedish Governmental Agency for Innovation Systems (VINNOVA) and the Knut & Alice Wallenberg Foundation through the project grant 3DEM-NATUR and a grant for purchasing the TEM. The research leading to these results has received funding from the European Union Seventh Framework Programme under Grant Agreement 312483 - ESTEEM2 (Integrated Infrastructure Initiative–I3).

Notes and references

[a] Berzelii Centre EXSELENT on Porous Materials and Inorganic and Structural Chemistry, Department of Materials and Environmental Chemistry, Stockholm University, SE-106 91 Stockholm, Sweden.

[b] Laboratorio de Microscopias Avanzadas (LMA), Instituto de Nanociencia de Aragon (INA), Universidad de Zaragoza, Mariano Esquillor, 50018 Zaragoza, Spain

† Electronic Supplementary Information (ESI) available: Plane group determination from the HAADF-STEM and HRTEM images, and comparison of crystallographic structure factors calculated from the structure model of silicalite-1 (MFI) with the amplitudes and phases extracted from the HAADF-STEM and HRTEM images. See DOI: 10.1039/b000000x/

1. E. Mugnaioli and U. Kolb, *Micropor. Mesopor. Mater.*, 2013, **166**, 93-101.

2. T. Willhammar, Y. F. Yun and X. D. Zou, *Adv. Funct. Mater.*, 2014, **24**, 182-199.
3. X. D. Zou, S. Hovmöller and P. Oleynikov, *Electron Crystallography – Electron Microscopy and Electron Diffraction*, Oxford University Press, Oxford, 2011.
4. C. Baerlocher, F. Gramm, L. Massüger, L. B. McCusker, Z. B. He, S. Hovmöller and X. D. Zou, *Science*, 2007, **315**, 1113-1116.
5. F. Gramm, C. Baerlocher, L. B. McCusker, S. J. Warrender, P. A. Wright, B. Han, S. Bong-Hong, Z. Liu, T. Ohsuna and O. Terasaki, *Nature*, 2006, **444**, 79-81.
6. C. Baerlocher, D. Xie, L. B. Mccusker, S. J. Hwang, I. Y. Chan, K. Ong, A. W. Burton and S. I. Zones, *Nat. Mater.*, 2008, **7**, 631-635.
7. D. J. d. Rosier and A. Klug, *Nature*, 1968, **217**, 130-134.
8. S. Hovmöller, *Ultramicroscopy*, 1992, **41**, 121-135.
9. X. D. Zou, M. Sundberg, M. Larine and S. Hovmöller, *Ultramicroscopy*, 1996, **62**, 103-121.
10. X. D. Zou, Z. M. Mo, S. Hovmöller, X. Z. Li and K. H. Kuo, *Acta. Crytstallogr.*, 2003, **A59**, 526-539.
11. T. E. Weirich, R. Ramlau, A. Simon, S. Hovmöller and X. D. Zou, *Nature*, 1996, **382**, 144-146.
12. A. Corma, M. Moliner, A. Cantín, M. Díaz-Cabañas, J. Jordá, D. L. Zhang, J. L. Sun, K. Jansson, S. Hovmöller and X. D. Zou, *Chem. Mater.*, 2008, **20**, 3218-3223.
13. T. Ohsuna, Z. Liu, O. Terasaki, K. Hiraga and M. Camblor, *J. Phys. Chem. B*, 2002, **106**, 5673-5678.
14. J. L. Sun, Z. B. He, S. Hovmöller, X. D. Zou, F. Gramm, C. Baerlocher and L. B. McCusker, *Z. Kristallogr.*, 2010, **225**, 77-85.
15. T. Willhammar, J. L. Sun, W. Wan, P. Oleynikov, D. L. Zhang, X. D. Zou, M. Moliner, J. Gonzalez, C. Martinez, F. Rey and A. Corma, *Nat. Chem.*, 2012, **4**, 188-194.
16. B. Goris, S. Bals, W. V. d. Broek, E. Carbó-Argibay, S. Gómez-Graña, L. M. Liz-Marzán and G. V. Tendeloo, *Nat. Mater.*, 2012, **11**, 930-935.
17. C. C. Chen, C. Zhu, E. R. White, C.-Y. Chiu, M. C. Scott, B. C. Regan, L. D. Marks, Y. Huang and J. W. Miao, *Nature*, 2013, **496**, 74-77.
18. A. Mayoral, T. Carey, P. A. Anderson, A. Lubk and I. Diaz, *Angew. Chem. Int. Ed.*, 2011, **50**, 11230–11233.
19. A. Mayoral, T. Carey, P. A. Anderson and I. Diaz, *Micropor. Mesopor. Mater.*, 2013, **166**, 117-122.
20. A. Mayoral, J. Coronas, C. Casado, C. Tellez and I. Díaz, *Chem. Cat. Chem.*, 2013, **5**, 2595–2598.
21. V. Ortalan, A. Uzun, B. C. Gates and N. D. Browning, *Nature Nanotechnology*, 2010, **5**, 506-510.
22. C. Baerlocher and L. B. McCusker, http://www.iza-structure.org/databases/books/Atlas_6ed.pdf, 2011.
23. A. Mayoral, J. E. Readman and P. A. Anderson, *J. Phys. Chem. C*, 2013, **117**, 24485–24489.
24. P. Oleynikov, *Cryst. Res. Technol.*, 2011, **46**, 569-579.

TOC

The 3D atomic structure of silicalite-1 can be reconstructed for the first time by combining three high resolution HAADF-STEM images.